Alternating-current conductivity and dielectric properties of $Ge_{25}Sb_{15-x}Bi_xS_{60}$ bulk and thin-film glasses

2002 J. Phys.: Condens. Matter 14 1199

(http://iopscience.iop.org/0953-8984/14/6/307)

INSTITUTE OF PHYSICS PUBLISHING JOURNAL OF PHYSICS: CONDENSED MATTER

J. Phys.: Condens. Matter **14** (2002) 1199–1212 PII: S0953-8984(02)26167-6

Alternating-current conductivity and dielectric properties of $Ge_{25}Sb_{15-x}Bi_xS_{60}$ bulk and thin-film glasses

M M El-Samanoudy

Physics Department, Faculty of Education, Ain Shams University, Roxy, Cairo, Egypt

Received 26 June 2001, in final form 19 November 2001
Published 1 February 2002
Online at stacks.iop.org/JPhysCM/14/1199

Abstract

The effect of the replacement of antimony atoms by bismuth atoms on the electrical properties of compounds of the melt-quenched and thermally evaporated $Ge_{25}Sb_{15-x}Bi_xS_{60}$ ($x = 0$, 5, 10 and 15) chalcogenide system are reported for the first time. The results for the alternating-current (ac) conductivity σ_{ac} and the dielectric constant ϵ_1 of some bulk and thin-film samples of the four different compositions are presented over the temperature range 134–373 K and the frequency range 0.1–100 kHz. The ac conductivity increases with increase in the Bi content and deposition rate and decreases with increase in the film thickness. Its frequency exponent s exhibits strong temperature dependence. Analysis of the results in the light of the correlated barrier-hopping model for ac conduction reveals that electronic conduction takes place by single-polaron and bipolaron hopping processes at high and low temperatures respectively. The effects of composition, temperature, deposition rate and film thickness on the dielectric constant and the loss factor are studied. The dielectric constant and the loss factor are found to increase with increase of the Bi content and the deposition rate, especially at high temperatures and low frequencies. It is also found that increase in the film thickness leads to increase of the dielectric constant. The values of the electrical conductivity of the thin-film samples are higher by over one order of magnitude than those of the corresponding bulk samples, a fact that can be attributed to the higher density of defect states in the former.

1. Introduction

Due to their inherent scientific interest and applications in various fields, chalcogenide glasses have attracted a lot of attention from scientists and engineers. The study of thin films in particular is of considerable importance because of their possible applications in electronic and optoelectronic devices. Measurements of the frequency and temperature dependence of the ac conductivity and dielectric constant of amorphous chalcogenide semiconductors has

been extensively utilized for understanding the conduction process in those materials [1]. The method provides an estimate of the density of defect states at the Fermi level which participate in electronic transport, and contributes towards the understanding of their nature.

Amorphous germanium chalcogenide semiconductors generally have p-type electrical conduction, and their electrical properties are not significantly changed by the addition of impurities because of the presence of a pinned Fermi level in them. However, the addition of Bi in relatively high concentrations ($\geqslant$7% for Ge–Se [2, 3], $\geqslant$11% for Ge–S [4] and $\geqslant$3.5% for Ge–Te [5]) produces a structurally modified semiconductor and induces a p–n transition. Bhatnagar and Bhatia [6] interpreted the results of their measurements of the ac conductivity in $Ge_{20}S_{80-x}Bi_x$ on the basis of the correlated barrier-hopping (CBH) model, showing that electronic conduction at $x = 0$ and 4 takes place via bipolaron hopping, whereas addition of Bi in higher concentrations ($x = 11$ and 15) leads to defect centres of a new type, which take part in a process of conduction by single-polaron hopping. Some of the electrical and optical properties of Ge–S–Bi have also been studied [7]. It was also shown [8] that the addition of lead, which is close to bismuth in the periodic table, induces a p–n transition in Ge–Se glasses.

It has further been shown that increasing the Bi concentration in $Ge_{20}Sb_{25-x}Bi_xSe_{55}$ ($0 \leqslant x \leqslant 15$) thin films leads to a p–n transition at some value of x between 5 and 10 [9]. The authors of [9] discussed their results on the dc electrical conductivity, thermoelectric power and the appearance of n-type conduction in terms of the chemical bonds formed in the films and related them to the defect states which appear as a result of the incorporation of Bi in high concentrations. The ac measurements were interpreted by assuming CBH of carriers between charged defect centres.

Some electrical, optical and physical properties of $Ge_{20}Sb_{15-x}Bi_xS_{65}$ ($0 \leqslant x \leqslant 15$) glasses have been studied [10]. The basic experimental findings of this work can be summarized as follows: with increasing concentration of Bi atoms, the optical gap decreases and the dc electrical conductivity increases, and for $x > 5$ a transition from p-type to n-type conduction is observed.

The purpose of the present investigation is to study the effect of the replacement of Sb atoms by Bi atoms on the electrical properties of bulk and thin-film samples from the $Ge_{25}Sb_{15-x}Bi_xS_{60}$ system. This paper deals with the frequency and temperature dependence of the ac conductivity and the dielectric constant of samples having different compositions, thicknesses and deposition rates. We expect this to shed some light on the conduction mechanism in the chalcogenide glasses which are chemically modified by Bi atoms. There is no detailed study of the electronic properties of this system reported in the literature, except for the ac conductivity measurements on $Ge_{20}Bi_{15}S_{65}$ [6].

2. Experimental procedure

The bulk glass materials $Ge_{25}Sb_{15-x}Bi_xS_{60}$ ($x = 0$, 5, 10 and 15) were prepared by the conventional melt-quenching technique. High-purity (99.999) materials were weighed according to their atomic percentage and were sealed in evacuated silica tubes under a pressure of 10^{-5} Torr. The sealed tubes were heated in a suitable furnace where the temperature was raised at a rate of 3–4 K min^{-1} up to 1273 K and kept around that temperature for 20 h during which the melt was continuously agitated to achieve homogenization. The tube was finally quenched in granulated ice.

Films of various compositions, deposition rates in the range 0.61–2.65 nm s^{-1} and thicknesses in the range 55.8–598.2 nm were prepared by thermal evaporation under vacuum (10^{-5} Torr) of the prepared compounds onto cleaned glass substrates kept at room temperature

using an Edwards E306 A coating unit. The film thickness and the deposition rate were measured during deposition using an Edward FTM 4 thickness monitor. The thickness values were later checked by using a multiple-beam interferometric method [11].

Structural analysis was carried out on samples by means of a Philips 3700 X-Pert x-ray powder diffractometer using nickel-filtered Kα copper radiation ($\lambda = 1.542$ Å). Differential scanning calorimetry (DSC) of bulk glasses was carried out using a Shimadzu model D-50 with a uniform heating rate of 10 K min^{-1}.

The chemical composition of both bulk and thin-film samples was determined by carrying out energy-dispersive spectroscopy (EDX) on a Joel 6400 scanning electron microscope with link-exl EDS detector. The acquired data were processed through a Zaf correction program which is a part of the link-exl package.

The electrical properties were measured in an especially designed cryostat under a vacuum of 10^{-3} Torr. The temperature measurements were facilitated by mounting the thermocouple very close to the sample. The measurements were carried out with sandwich structures using gold electrodes for thin-film samples and a highly conductive silver paste for the polished bulk samples which had thickness in the range 0.45–0.6 mm. Measurements of the capacitance C and the loss tangent $\tan\delta$ in the frequency range 0.1–100 kHz were carried out at various temperatures in the range 134–373 K by means of a Philips PM 6304 programmable automatic LCR meter. The dielectric constant ϵ_1 was calculated from the standard relation $C = \epsilon_1\epsilon_0 A/d$, where A is the cross-sectional area of the sample, d its thickness, C its capacitance and ϵ_0 the permittivity of free space. The dc conductivity was measured using a Keithley 617 C electrometer. Three measurements were made for each sample in order to check the reproducibility of the results.

3. Results

3.1. Characterization

Powder x-ray diffraction patterns of the prepared bulk compositions and their thin films have been measured to ascertain the non-crystalline nature of the material. The presence of only broad features and the absence of any sharp peaks in the diffractograms are taken as evidence for the amorphous nature of the bulk and thin-film samples. Samples with $x = 15$ have shown some traces of microcrystallites.

The composition of bulk and thin-film samples has been determined using EDX. Although the compositions of the thin films are not necessarily exactly the same as those of the starting bulk alloys, the relative concentrations of the constituent elements (Ge, Sb, Bi and S) in various thin films prepared by thermal evaporation at a deposition rate of 1.42 nm s^{-1} have been found to be more or less the same as those of the starting bulk alloys. A comparison of the compositions of some bulk and thin-film samples of the $Ge_{25}Sb_{15-x}Bi_xS_{60}$ chalcogenide system is given in table 1.

Table 1. A comparison of the compositions of some bulk samples and the thin-film samples prepared from them by thermal evaporation.

Bulk				Thin film			
Ge	Sb	Bi	S	Ge	Sb	Bi	S
25.11	15.45	—	59.44	24.69	15.21	—	60.11
24.66	10.32	5.23	59.79	24.66	10.19	5.01	60.14
25.16	5.20	10.08	59.56	25.67	5.11	9.55	59.67
25.26	—	14.59	60.15	25.42	—	14.15	60.43

DSC has been utilized to study the thermal properties of the prepared samples. The values of the glass transition temperature T_g of several samples were determined and these are listed in table 2.

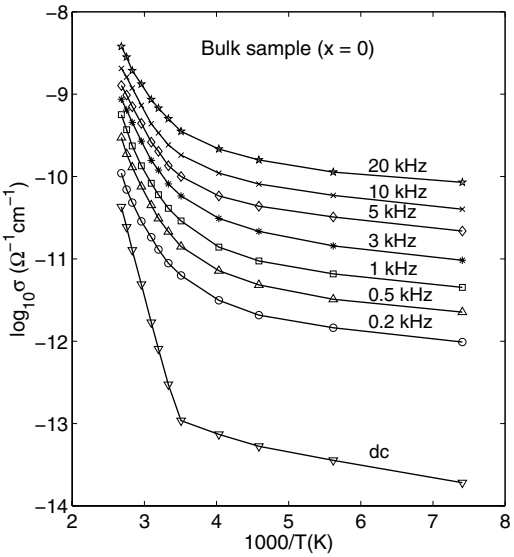

Figure 1. The temperature dependence of the dc conductivity and the total measured conductivity σ in an amorphous $Ge_{25}Sb_{15}S_{60}$ bulk sample at various frequencies.

Table 2. Values of the parameters used in the calculations, and the results: x is the bismuth content, T_g is the glass transition temperature, ϵ_1 is the dielectric constant (at $f = 10$ kHz), s is the ac conductivity frequency exponent (at $T = 300$ K), $\tan\delta$ is the loss tangent (at $T = 300$ K), W_m is the maximum barrier height, n is the number of electrons hopping between two sites, N is the total density of charged defect states, and N_p is the total density of localized states to which electrons may hop.

					NN_p (cm^{-6})		W_m (eV)	
x	T_g	s	$\tan\delta$	ϵ_1	$n = 1$	$n = 2$	$n = 1$	$n = 2$
Bulk								
0	589	0.89	0.004	16.48	5.99×10^{38}	1.29×10^{36}	1.12	2.64
5	572	0.85	0.039	19.82	1.77×10^{41}	1.11×10^{40}	0.99	2.56
10	563	0.78	0.084	28.20	4.83×10^{41}	3.05×10^{40}	0.86	2.52
15	555	0.71	0.148	32.32	7.82×10^{41}	2.38×10^{40}	0.79	2.50
Thin film								
0	589	0.74	0.171	5.02	1.43×10^{39}	8.08×10^{36}	1.04	2.63
5	572	0.68	0.298	12.94	3.77×10^{41}	1.23×10^{40}	0.98	2.56
10	563	0.61	0.651	15.58	8.06×10^{41}	2.86×10^{40}	0.95	2.57
15	555	0.55	2.140	19.56	1.55×10^{43}	2.70×10^{40}	0.93	2.52

3.2. Frequency and temperature dependence of the ac conductivity

Experimental results on the temperature dependence of the total measured conductivity $\sigma(\omega)$ have been obtained. Figure 1 shows this dependence for an amorphous $Ge_{25}Sb_{15}S_{60}$ bulk

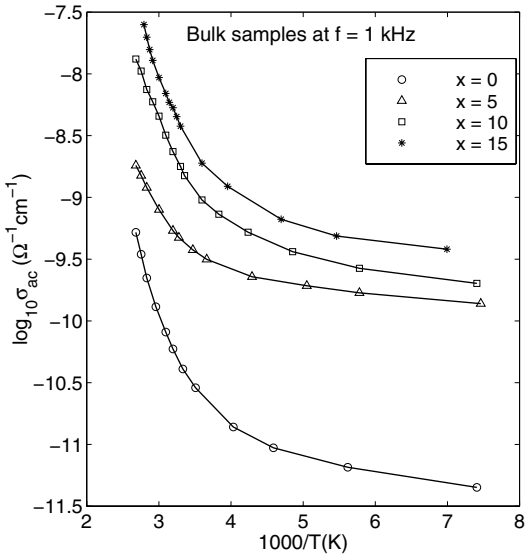

Figure 2. The temperature dependence of σ_{ac} at $f = 1$ kHz for $Ge_{25}Sb_{15-x}Bi_xS_{60}$ ($x = 0$, 5, 10 and 15) amorphous bulk samples.

sample at various frequencies as a representative example. The corresponding temperature dependence of the dc conductivity σ_{dc} is also plotted in the figure.

At all compositions, a significant change in the temperature dependence of $\sigma(\omega)$ takes place. At low temperatures, only a small increase in $\sigma(\omega)$ with temperature at any fixed frequency is observed. At higher temperatures, σ exhibits a comparatively faster rise with increasing temperature. The onset of the faster rise in $\sigma(\omega)$ is found to shift slightly towards higher temperatures as the frequency is increased.

The ac conductivity σ_{ac} is defined by

$$\sigma_{ac}(\omega) = \sigma(\omega) - \sigma_{dc} \tag{1}$$

where σ_{dc} is the dc conductivity measured at the same temperature as $\sigma(\omega)$. The effect of composition on the temperature dependence of σ_{ac} at $f = 1$ kHz is shown in figure 2 for bulk glasses.

A feature common to almost all amorphous semiconductors and some other disordered systems is that the ac conductivity σ_{ac} increases with increasing frequency, at least in the range $10\ s^{-1} < \omega < 10^8\ s^{-1}$, according to the power-law relation

$$\sigma_{ac}(\omega) = A\omega^s \tag{2}$$

where A is a constant and the frequency exponent s is $\leqslant 1$.

The frequency dependence of $\sigma_{ac}(\omega)$ for all compositions at various temperatures is found to nicely follow equation (2). As an example, a typical set of plots of $\sigma_{ac}(\omega)$ against $\log f$ for $Ge_{25}Sb_{10}Bi_5S_{60}$ bulk samples are shown in figure 3. It is clear from the figure that $\sigma_{ac}(\omega)$ increases with increasing frequency and temperature.

The effect of composition on the frequency dependence at $T = 303$ K of $\sigma_{ac}(\omega)$ for amorphous $Ge_{25}Sb_{15-x}Bi_xS_{60}$ 120 nm thin films deposited at a rate of 1.42 nm s^{-1} is shown in figure 4. It can be seen from figures 2 to 4 that σ_{ac} increases as the Bi content increases. It also increases with the increase in temperature, with $\sigma_{ac}(\omega)$ in thin films being higher than that in the corresponding bulk samples.

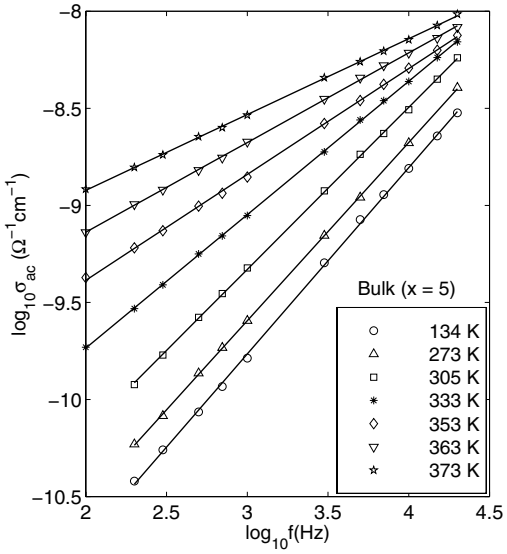

Figure 3. The frequency dependence of the ac conductivity σ_{ac} of a $Ge_{25}Sb_{10}Bi_5S_{60}$ amorphous bulk sample at various temperatures.

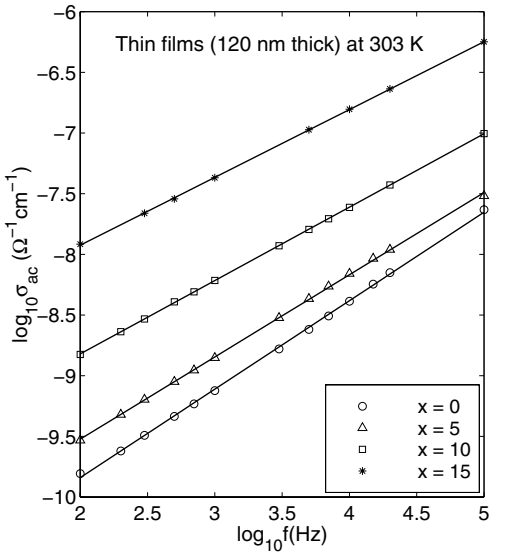

Figure 4. The effect of composition on the frequency dependence of the ac conductivity at 303 K of amorphous $Ge_{25}Sb_{15-x}Bi_xS_{60}$ 120 nm thin films deposited at a rate of 1.42 nm s^{-1}.

The frequency exponent s has been calculated from the slope of the straight-line relation between $\log \sigma_{ac}$ and $\log f$ and is plotted as a function of temperature in figure 5 for some bulk glass samples. As can be seen from those figures, s is smaller than unity at low temperatures and decreases with increasing temperature. Values of s of some samples at $T = 300$ K are listed in table 2.

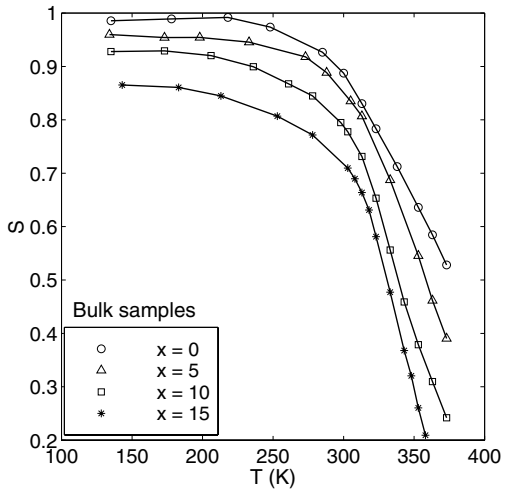

Figure 5. The effect of composition on the temperature dependence of the experimental values of the exponent s as determined from the straight-line relationship between $\log \sigma_{ac}$ and $\log f$ for $Ge_{25}Sb_{15-x}Bi_xS_{60}$ bulk samples.

Table 3. The effect of the deposition ('Dep.') rate on the dc, ac and dielectric properties of the compositions ('Comp.') $Ge_{25}Sb_5Bi_{10}S_{60}$ (listed as 'A') and $Ge_{25}Sb_{15}S_{60}$ (listed as 'B') of thin films at 300 K: σ_{dc} is the dc conductivity, σ_{ac} is the ac conductivity, ϵ_1 is the dielectric constant (at $f = 10$ kHz), s is the ac conductivity frequency exponent, $\tan\delta$ is the loss tangent (at $T = 300$ K), W_m is the maximum barrier height, n is the number of electrons hopping between two sites, N is the total density of charged defect states, and N_p is the total density of localized states to which electrons may hop.

Comp.	Dep. rate (nm s^{-1})	σ_{dc} (Ω^{-1} cm^{-1})	σ_{ac} (Ω^{-1} cm^{-1})	s	$\tan\delta$	ϵ_1	NN_p (cm^{-6})		W_m (eV)	
							$n = 1$	$n = 2$	$n = 1$	$n = 2$
A	0.62	3.36×10^{-11}	5.14×10^{-9}	0.62	0.156	13.73	8.89×10^{40}	7.31×10^{39}	0.95	2.56
	1.42	8.19×10^{-11}	7.95×10^{-9}	0.61	0.651	15.58	8.06×10^{41}	2.86×10^{40}	0.95	2.57
	2.65	1.49×10^{-10}	1.67×10^{-8}	0.55	1.126	22.54	1.33×10^{42}	9.28×10^{40}	0.93	2.55
B	0.61	2.91×10^{-12}	5.68×10^{-10}	0.75	0.153	4.95	9.23×10^{38}	2.70×10^{38}	1.09	2.62
	1.42	3.19×10^{-12}	6.36×10^{-10}	0.74	0.171	5.02	1.43×10^{39}	8.08×10^{36}	1.04	2.63
	1.96	7.94×10^{-12}	9.88×10^{-10}	0.71	0.223	6.28	6.16×10^{39}	8.92×10^{36}	1.02	2.60
	2.65	1.27×10^{-11}	2.34×10^{-9}	0.67	0.499	7.43	2.99×10^{40}	2.40×10^{37}	1.01	1.91

The frequency and temperature dependences of σ_{ac} for thin-film samples deposited at various deposition rates between 0.61 and 2.65 nm s^{-1} and having different thicknesses were investigated. Figure 6 shows the effect of deposition rate on the temperature dependence of σ_{ac} at 1 kHz for $Ge_{25}Sb_5Bi_{10}S_{60}$ 120 nm thin film. Values of s for some thin-film samples are listed in tables 3 and 4. We see from the figure and tables that the ac conductivity increases with increasing deposition rate and decreasing film thickness.

3.3. Frequency and temperature dependence of the dielectric constant ϵ_1 and loss tangent $\tan\delta$

The temperature and frequency dependence of the dielectric constant ϵ_1 and the loss tangent $\tan\delta$ for the glassy alloys $Ge_{25}Sb_{15-x}Bi_xS_{60}$ ($x = 0$, 5, 10 and 15) were studied in the

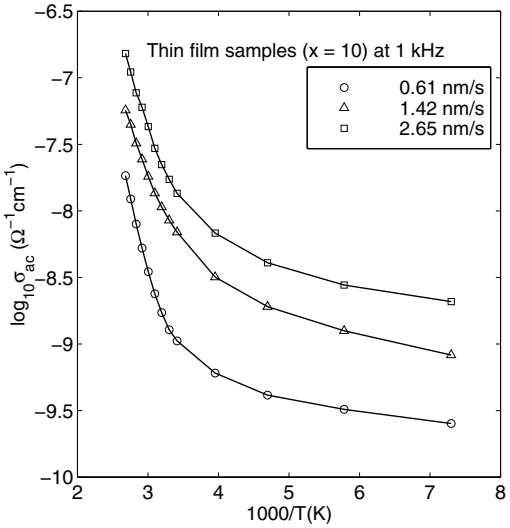

Figure 6. The temperature dependence of σ_{ac} in $Ge_{25}Sb_5Bi_{10}S_{60}$ 120 nm thin films of various deposition rates at $f = 1$ kHz.

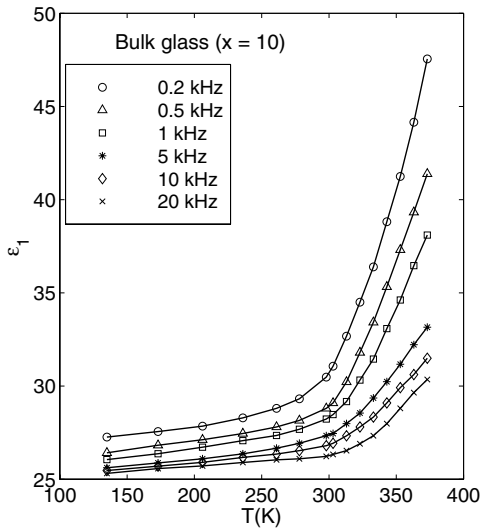

Figure 7. The temperature dependence of the dielectric constant ϵ_1 of a $Ge_{25}Sb_5Bi_{10}S_{60}$ bulk sample at various frequencies.

temperature range 134–373 K and the frequency range 0.1–100 kHz. The variation of the dielectric constant with temperature at various frequencies for a $Ge_{25}Sb_5Bi_{10}S_{60}$ bulk sample is shown in figure 7 as an example. It is observed that the dielectric constant is strongly temperature dependent at lower frequencies, but its temperature dependence gets weaker as the frequency increases. The dielectric constant decreases with increasing frequency, and the decrease is sharper at lower frequencies and higher temperatures.

The effect of composition on the temperature dependence of ϵ_1 for bulk samples at $f = 1$ kHz and $T = 303$ K is shown in figure 8. The temperature dependence of ϵ_1 for samples with $x = 0$ and 5 is relatively weak, but the samples with $x = 10$ and 15 exhibit

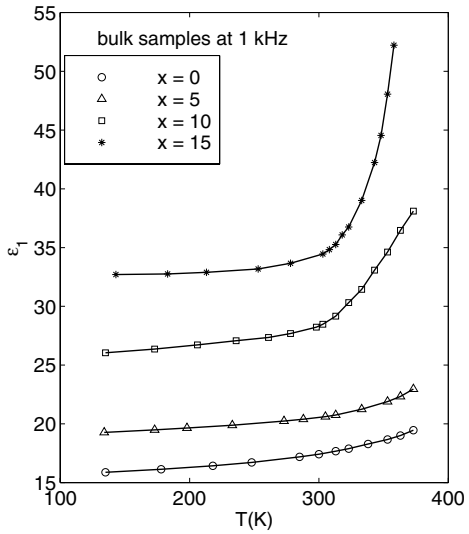

Figure 8. The effect of composition on the temperature dependence of the dielectric constant ϵ_1 of amorphous $Ge_{25}Sb_{15-x}Bi_xS_{60}$ bulk samples at 1 kHz.

Table 4. The effect of the film thickness on the dc, ac and dielectric properties of $Ge_{25}Sb_{15}S_{60}$ thin films for deposition rate 1.42 nm s^{-1}: σ_{dc} is the dc conductivity, σ_{ac} is the ac conductivity, ϵ_1 is the dielectric constant (at $f = 1$ kHz), s is the ac conductivity frequency exponent, $\tan\delta$ is the loss tangent (at $T = 300$ K), W_m is the maximum barrier height, n is the number of electrons hopping between two sites, N is the total density of charged defect states and N_p is the total density of localized states to which electrons may hop.

Thickness (nm)	σ_{dc} (Ω^{-1} cm^{-1})	σ_{ac} (Ω^{-1} cm^{-1})	s	$\tan\delta$	ϵ_1	NN_p (cm^{-6})		W_m (eV)	
						$n = 1$	$n = 2$	$n = 1$	$n = 2$
55.8	2.92×10^{-11}	1.95×10^{-9}	0.71	0.665	5.05	2.83×10^{39}	3.25×10^{37}	0.98	1.95
128.6	3.19×10^{-12}	6.36×10^{-10}	0.74	0.171	6.91	1.78×10^{39}	1.01×10^{37}	1.06	2.68
223.1	1.31×10^{-12}	3.65×10^{-10}	0.75	0.078	8.14	9.91×10^{38}	1.92×10^{37}	1.04	2.65
330.8	9.73×10^{-13}	2.53×10^{-10}	0.75	0.043	9.52	1.85×10^{39}	5.15×10^{36}	1.08	2.68
465.5	8.15×10^{-13}	2.33×10^{-10}	0.76	0.038	11.04	—	—	—	—
598.2	5.97×10^{-13}	2.00×10^{-10}	0.78	0.029	12.54	9.01×10^{39}	6.26×10^{35}	1.06	0.92

stronger temperature dependence at temperatures above about 290 K. It is observed that the dielectric constant increases with the Bi content of the samples.

The variation of the dielectric constant ϵ_1 with frequency and temperature for thin films of various compositions, thicknesses and deposition rates has been investigated. Figure 9 shows the effect of film thickness on the frequency dependence at $T \simeq 303$ K of ϵ_1 for $Ge_{25}Sb_{15}S_{60}$ thin films. Some values of ϵ_1 for bulk and thin-film samples are given in tables 2–4. It can be seen from table 3 that the dielectric constant increases as the deposition rate increases from 0.61 to 2.65 nm s^{-1}.

Figure 10 shows the temperature dependence of $\tan\delta$ for a $Ge_{25}Bi_{15}S_{60}$ bulk glass sample at several frequencies. It can be seen from the figure that $\tan\delta$ exhibits strong temperature and frequency dependence. Values of $\tan\delta$ at 1 kHz for various compositions, deposition rates and film thicknesses have been measured and these are listed in tables 2–4. It is observed that the values of $\tan\delta$ are much greater for the samples with $x = 15$ than for samples with $x = 0$, 5 and 10, and that $\tan\delta$ is generally greater in thin-film samples.

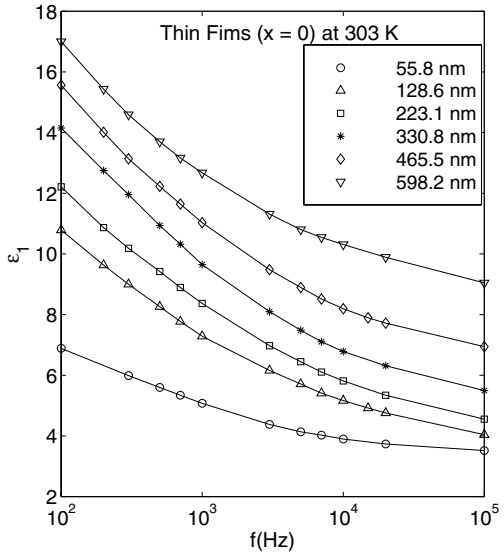

Figure 9. The frequency dependence of the dielectric constant ϵ_1 at 303 K of $Ge_{25}Sb_{15}S_{60}$ amorphous thin films of various thicknesses deposited at a rate of 1.42 nm s^{-1}.

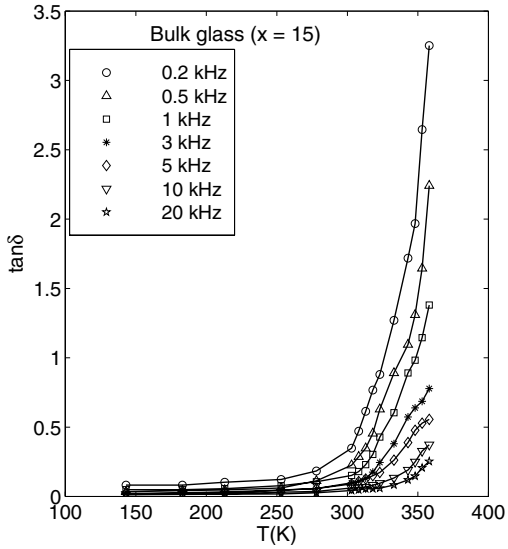

Figure 10. The temperature dependence of tan δ for $Ge_{25}Bi_{15}S_{60}$ bulk glass at various frequencies.

4. Analysis and discussion

4.1. The ac conductivity

The frequency dependence of the ac conductivity of amorphous and disordered materials (equation (2)) has been ascribed to the relaxation caused by the motion of electrons or holes tunnelling or hopping between equilibrium sites [1]. According to the quantum-mechanical tunnelling (QMT) model, the exponent s is almost equal to 0.8 and increases slightly with

increasing temperature. In most of the chalcogenide glasses, the values of s range from 0.7 to 1.0 at room temperature and have a tendency to decrease with increasing temperature [12]. Therefore, the QMT model is considered not applicable to those materials, and the CBH model [13] has been extensively applied to chalcogenide glassy semiconductors. In this model CBH of bipolarons (two electrons hopping between charged defect states D^+ and D^-) has been proposed [13, 14] to interpret the frequency dependence of conductivity in chalcogenide glasses as given by equation (2). The theory has explained many low-temperature features, particularly the temperature-dependent values of the parameters A and s. However, it does not predict the strong temperature dependence of σ_{ac} which has been observed at higher temperature, particularly in the low-frequency range. Shimakawa [15] has suggested that, at higher temperatures, the D^0 neutral defect states are produced by thermal excitation of D^+ and D^- states, and thus single-polaron hopping (an electron hopping between D^0 and D^+ or a hole hopping between D^0 and D^-) becomes the dominant process.

In the CBH model, electrons in charged defect states hop over the coulombic barrier whose height W (in SI units) is given by

$$W = W_m - \frac{ne^2}{\pi\epsilon_1\epsilon_0 r} \tag{3}$$

where W_m is the maximum barrier height, e is the electronic charge, ϵ_1 is the bulk dielectric constant, r is the distance between the hopping sites and n is the number of electrons that hop between two defect sites ($n = 1$ or 2 for single-polaron and bipolaron processes respectively).

The relaxation time τ for electrons to hop over a barrier of height W is given by

$$\tau = \tau_0 \exp\left(\frac{W}{kT}\right) \tag{4}$$

where τ_0 is a characteristic relaxation time of the order of an atomic vibrational period, T is the sample temperature and k is Boltzmann's constant.

The ac conductivity $\sigma_{ac_2}(\omega)$ originating from intimate D^+D^- defect pairs having non-random distribution [13, 14] can be written as

$$\sigma_{ac_2}(\omega) = \frac{n\pi^3\epsilon_1\epsilon_0 N N_p \omega R_\omega^6}{6} \exp\left(\frac{e^2}{4\pi\epsilon_0\epsilon_1 k T_g R_\omega}\right) \tag{5}$$

where N is the density of localized states at which electrons exist, N_p is the density of localized states to which electrons hop, T_g is the glass transition temperature, and R_ω is the optimum hopping distance which is given by

$$R_\omega = \frac{ne^2}{\pi\epsilon_1\epsilon_0 W_m}\left(1 + \frac{kT}{W_m}\ln(\tau_0\omega)\right)^{-1}. \tag{6}$$

The exponent s_2 derived from equations (5) and (6) is given by

$$s_2 = 1 + \left(\frac{1}{8T_g} - \frac{6\pi\epsilon_1\epsilon_0 k}{2e^2}R_\omega\right)T \tag{7}$$

where $n = 2$ and 1 for the bipolaron and single-polaron hopping processes respectively.

The ac conductivity $\sigma_{ac_1}(\omega)$ for single-polaron hopping originating from randomly distributed defect centres [1, 13] can be expressed as

$$\sigma_{ac_1}(\omega) = \frac{\pi^3\epsilon_1\epsilon_0 N N_p \omega R_\omega^6}{6} \tag{8}$$

where R_ω is still given by equation (6), with $n = 1$. The corresponding expression for the exponent s_1 for single-polaron hopping is

$$s_1 = 1 - \frac{6kT}{W_m}. \tag{9}$$

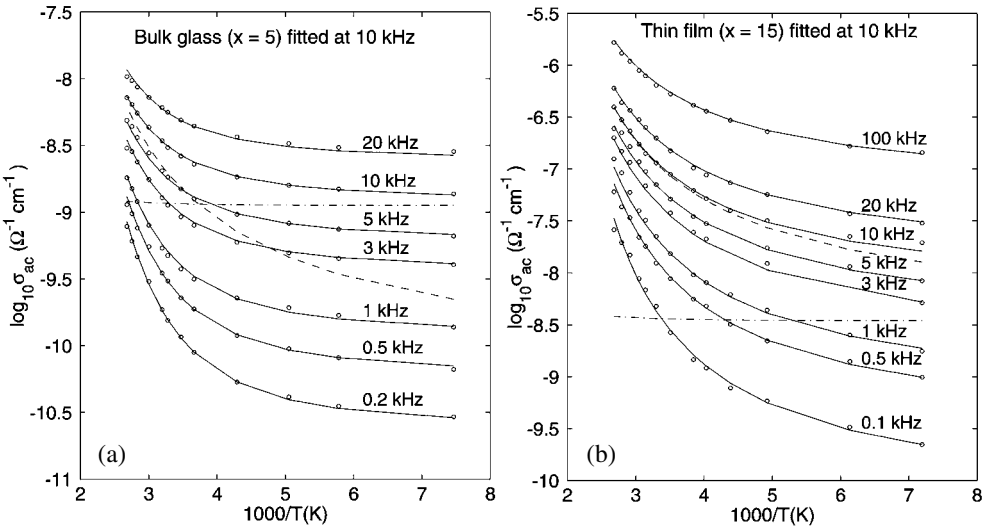

Figure 11. The CBH model fitting to the temperature dependence of the ac conductivity σ_{ac} at various frequencies in (a) $Ge_{25}Sb_{10}Bi_5S_{60}$ bulk glass and (b) $Ge_{25}Bi_{15}S_{60}$ amorphous thin film prepared at a deposition rate of 1.42 nm s^{-1}. The values of σ_{ac_1} and σ_{ac_2} calculated from equation (8) (with $n = 1$) and equation (5) (with $n = 2$) are shown as the broken (– – –) and chain (— · —) curves respectively. The sum $\sigma_{ac_1} + \sigma_{ac_2}$ is shown by continuous curves (——). The open circles represent data points.

Fits to our experimental data have been made assuming that σ_{ac} in the $Ge_{25}Sb_{15-x}Bi_xS_{60}$ system receives a contribution from the two conduction processes described above such that $\sigma_{ac} = \sigma_{ac_1} + \sigma_{ac_2}$, where σ_{ac_1} and σ_{ac_2} are the ac conductivities for single polarons as given by equation (8) and for bipolarons as given by equation (5) (with $n = 2$) respectively. The product NN_p and the maximum barrier height W_m are treated as parameters to be determined from the least-squares error fit to the experimental plots of $\log \sigma_{ac}$ against $1/T$. The fitting is done at one frequency (10 kHz) and the same values of the fitting parameters are used for the other frequencies. The dielectric constant ϵ_1 has been estimated from the measured capacitive component of the samples. The glass transition temperature T_g was determined from the DSC measurements. Since the $x = 15$ samples show double glass transitions, we have used the lower glass transition temperature in the calculation. The various parameters used in the fitting procedure for various compositions, deposition rates and thicknesses are summarized in tables 2 to 4.

Figures 11(a) and (b) show respectively a typical set of plots of the computed $\log \sigma_{ac}$ as a function of $1/T$ for a $Ge_{25}Sb_{10}Bi_5S_{60}$ bulk glass and a $Ge_{25}Bi_{15}S_{60}$ amorphous thin film prepared at a deposition rate of 1.42 nm s^{-1}. The broken and chain curves show the calculated contributions from the single-polaron and bipolaron hopping processes respectively, while their sum is indicated by the continuous curves in the figures. Open circles represent experimental data points for σ_{ac}. The calculated curves agree with the experimental results for all the measured frequencies to within about 10%. The parameters obtained from fitting the CBH model to the data, namely the defect density product NN_p and the maximum barrier height W_m, are also summarized in tables 2 to 4.

The results show that the two processes of electric conduction by bipolaron hopping between non-randomly distributed defect sites and single-polaron hopping between randomly distributed defect sites are present in all the four compositions, with the former process predominating at lower temperatures and the latter at higher temperatures. The situation

here is similar to that for many other chalcogenide glasses which contain bismuth or lead and exhibit p–n transitions [6, 15–19].

The ac conductivity data exhibit the marked effect of the Bi-induced impurity states, particularly in samples with $x = 10$ and 15. With the addition of a small quantity of Bi impurity, the density of the defects taking part in both bipolaron and single-polaron hopping conduction increases. Going back to figure 2, we see that the values of σ_{ac} in samples with $x = 5$ are over one order of magnitude higher than those in the $x = 0$ samples. Further increase in the Bi concentration leads to a faster increase in the density of the defects responsible for single-polaron hopping than in the density of those responsible for bipolaron hopping. This is an interesting feature of these amorphous semiconductors.

Tables 2–4 also show that the values of the defect density product NN_p for thin films are higher than those for bulk samples. It is reasonable to assume that the thin films contain an increased number of homonuclear bonds in comparison with the chemically ordered bulk samples which were prepared from the melt [20]. Since film growth takes place at temperatures below the melting point of the material, the ordering processes are hindered. Moreover, one cannot expect molecules occurring in the vapour states to be identical with the short-range configurations of a melt of an identical composition. In fact, through analysing extended x-ray absorption fine-structure (EXAFS) and Raman spectroscopy results by means of various models, Nemanich *et al* [21, 22] concluded that evaporated As_2Se_3 and $GeSe_2$ contain a fairly large fraction of homonuclear bonds in contrast to the corresponding bulk glasses. From these results the structure of evaporated $Ge_{25}Sb_{15-x}Bi_xS_{60}$ thin films can be assumed to be chemically disordered and to contain a large number of wrong bonds, although the average composition is the same as that of the corresponding bulk samples.

4.2. Dielectric relaxation

The complex dielectric constant ϵ of a material can be written as $\epsilon = \epsilon_1 + i\epsilon_2$ where ϵ_1 is the real part (dielectric constant) and ϵ_2 the imaginary part (dielectric loss), in terms of which the loss tangent $\tan\delta$ is defined as $\tan\delta = \epsilon_2/\epsilon_1$. The dielectric loss ϵ_2 is related to the ac conductivity by [13]

$$\sigma_{ac}(\omega) = \omega\epsilon_0\epsilon_2(\omega).$$

The experimental data for the unmodified and low-Bi samples ($x = 0$ and 5 respectively) indicate that the polarization of the medium has a weak temperature dependence, and that the centres responsible for dielectric relaxation undergo little movement below about 300 K. The polarization of the samples undergoes a significant change as the Bi concentration is further increased in the bulk glasses or their thin films. With $x = 10$ and 15, both ϵ_1 and $\tan\delta$ exhibit strong temperature dependence at higher temperatures.

The temperature and frequency dependence of the dielectric constant (figure 7) reveal that dielectric polarization results from molecular dipoles [23, 24], which remain frozen at lower temperature ($T < T_c$) and attain rotational freedom at higher temperatures ($T > T_c$) when the effect of the molecular interaction energy becomes weaker than that of the thermal energy [25]; thereafter the dielectric constant varies exponentially with temperature.

The origin of molecular dipoles may be linked to micro-inhomogeneities, the large polarizability of Bi atoms [26] and the formation of microclusters [27]. The intimate valence-alternation pairs formed by the Coulomb attraction between charged C_3^+ and C_1^- defects have also been proposed as the sources of molecular dipoles in chalcogenide glasses containing bismuth [28].

The noticeable change of slope in the $\tan\delta$–T plot for an $x = 15$ sample (figure 10) may indicate the presence of a weak, Debye-like loss peak [1, 29] which may be attributed to the movement and relaxation of the Bi-induced paired defect states under the effect of an applied ac field.

5. Conclusions

We have investigated for the first time the electronic conduction process in the amorphous $Ge_{25}Sb_{15-x}Bi_xS_{60}$ system which exhibits a p–n transition, by measuring the frequency and temperature dependence of the ac conductivity and dielectric constant.

Analysis of the results based on the CBH model reveals that the electronic conduction in the system could be described by a combination of bipolaron and single-polaron hopping processes, with the former predominating at lower temperatures and the latter at higher temperatures. The energy barrier height and the densities of the defect states are deduced from a comparison between the theoretical and experimental results.

The dielectric constant and the loss tangent are frequency and temperature dependent and increase as the Bi content and deposition rate increase. It is reasonable to assume that the number of homonuclear bonds in the thin films is higher than that in the chemically ordered bulk samples prepared from the melt.

Acknowledgments

I thank Dr M M Elocker and Dr H Talaat for allowing me to use the facilities of their Laboratory at Al-Azhar University.

References

[1] Elliott S R 1987 *Adv. Phys.* **36** 135
[2] Tohge N, Minami T, Yamamato Y and Tanaka M 1980 *J. Appl. Phys.* **51** 1048
[3] Nagels P, Rotti M and Vikhrov W 1981 *Phys. Colloq. C* **4** 907
[4] Nagels P, Tichy L, Triska A and Ticha H 1983 *J. Non-Cryst. Solids* **59–60** 1015
[5] Bhatia K L, Parthasarathy G, Sharma A K and Gopal E S R 1988 *Phys. Rev.* B **38** 6342
[6] Bhatnagar V K and Bhatia K L 1990 *J. Non-Cryst. Solids* **119** 214
[7] Sedeek K, Fadel M and Afifi M A 1998 *J. Mater. Sci.* **33** 4621
[8] Tohge N, Matsuo H and Minami T 1987 *J. Non-Cryst. Solids* **95–96** 809
[9] Kumar R, Yoshida A and Mehra R M 1991 *J. Non-Cryst. Solids* **130** 248
[10] Malek J, Klikorka J, Benes L, Tichy L and Triska A 1986 *J. Mater. Sci.* **21** 488
[11] Tolansky S 1970 *Multiple-Beam Interference Microscopy of Metals of Surface and Films* (London: Academic) p 55
[12] Long A R 1982 *Adv. Phys.* **31** 553 and references therein
[13] Elliott S R 1977 *Phil. Mag.* B **36** 1291
[14] Elliott S R 1978 *Phil. Mag.* B **37** 553
[15] Shimakawa K 1982 *Phil. Mag.* B **46** 123
[16] Bhatia K L, Malik S K, Kishore N and Singh S P 1992 *Phil. Mag.* B **66** 587
[17] Singh M, Bhatia K L, Kishore N, Singh P and Kundu R S 1995 *J. Non-Cryst. Solids* **180** 251
[18] Bhatia K L, Singh M, Kishore N and Suzuki M 1996 *Phil. Mag.* B **73** 383
[19] Malik S K, Bhatia K L and Bhatnagar V K 1991 *Phil. Mag.* B **63** 573
[20] Watanabe I, Maeda T and Shimizu T 1980 *J. Non-Cryst. Solids* **37** 335
[21] Nemanich R J, Connell G A N, Hayes T M and Street R A 1978 *Phys. Rev.* B **18** 6900
[22] Street R A, Nemanich R J and Connell G A N 1978 *Phys. Rev.* B **18** 6915
[23] Panwar O S, Radhakrishna M, Srivastava K K and Lakshminarayan K N 1980 *Phil. Mag.* B **41** 253
[24] Goel D K, Singh C P, Shukla R K and Kumar A 2000 *J. Mater. Sci.* **35** 1017
[25] Srivastava K K, Goyal D R, Kumar A, Lakshminarayan K N, Panwar O S and Krishan I 1977 *Phys. Status Solidi* a **41** 323
[26] Edel'man V S 1977 *Sov. Phys.–Usp.* **20** 819
[27] Phillips J C 1983 *J. Non-Cryst. Solids* **55** 179
[28] Kastner M, Adler D and Fritzsche H 1976 *Phys. Rev. Lett.* **37** 1504
[29] Isard J O 1970 *J. Non-Cryst. Solids* **4** 357